THE FASEB JOURNAL • RESEARCH • www.fasebj.org

Antibody-mediated blockade of JMJD6 interaction with collagen I exerts antifibrotic and antimetastatic activities

Silvia Miotti,* Alessandro Gulino,† Renata Ferri,* Mariella Parenza,* Agnieszka Chronowska,*,[1] Daniele Lecis,* Sabina Sangaletti,* Elda Tagliabue,‡ Claudio Tripodo,† and Mario P. Colombo*,[2]

*Molecular Immunology Unit and ‡Molecular Targeting Unit, Department of Experimental Oncology and Molecular Medicine, Fondazione Istituto di Ricovero e Cura a Carattere Scientifico (IRCCS) Istituto Nazionale dei Tumori, Milan, Italy; and †Tumor Immunology Unit, Department of Health Sciences, University of Palermo, Palermo, Italy

ABSTRACT: JMJD6 is known to localize in the nucleus, exerting histone arginine demethylase and lysyl hydroxylase activities. A novel localization of JMJD6 in the extracellular matrix, resulting from its secretion as a soluble protein, was unveiled by a new anti-JMJD6 mAb called P4E11, which was developed to identify new targets in the stroma. Recombinant JMJD6 binds with collagen type I (Coll-I), and distinct JMJD6 peptides interfere with collagen fibrillogenesis, collagen-fibronectin interaction, and adhesion of human tumor cells to the collagen substrate. P4E11 and collagen binding to JMJD6 are mutually exclusive because the amino acid sequences of JMJD6 necessary for the interaction with Coll-I are part of the conformational epitope recognized by P4E11. In mice injected with mouse 4T1 breast carcinoma cells, treatment with P4E11 reduced fibrosis at the primary tumor and prevented lung metastases. Reduction of fibrosis has also been documented in human breast and ovarian tumors (MDA-MB-231 and IGROV1, respectively) xenotransplanted into immunodeficient mice treated with P4E11. In summary, this study uncovers a new localization and function for JMJD6 that is most likely independent from its canonical enzymatic activities, and demonstrates that JMJD6 can functionally interact with Coll-I. P4E11 mAb, inhibiting JMJD6/Coll-I interaction, represents a new opportunity to target fibrotic and tumor diseases.—Miotti, S., Gulino, A., Ferri, R., Parenza, M., Chronowska, A., Lecis, D., Sangaletti, S., Tagliabue, E., Tripodo, C., Colombo, M. P. Antibody-mediated blockade of JMJD6 interaction with collagen I exerts antifibrotic and antimetastatic activities. FASEB J. 31, 5356–5370 (2017). www.fasebj.org

KEY WORDS: JmjC family · extracellular matrix · monoclonal antibody · *in vivo* treatment · peptide library

The variety of stromal cells and extracellular matrix (ECM) components contributes to the complexity of tumor microenvironment. ECM is constituted by secreted structural proteins including collagens, fibronectin (Fn), proteoglycans, and laminins, which form a network that provides mechanical support and controls cell proliferation, adhesion, and migration (1). Other components of ECM are constituted by matricellular proteins that, although not endowed with structural functions, contribute to the regulation of cell–ECM interactions. Among the matricellular proteins, the secreted protein acidic and rich in cysteine (SPARC) displays a pivotal function in ECM assembly, particularly of fibrillar collagen, and in Fn-induced integrin-linked kinase activation and signaling (2). Other secreted proteins that belong to the lysyl oxidase family are involved in the formation of covalent intra- and intermolecular cross-links between collagen secreted microfibrils (3), which increase matrix stiffness and tumor progression (4, 5).

Collagen post-translational modifications start during its biosynthesis, which occurs inside the endoplasmic reticulum. The Fe^{2+}- and 2-oxoglutarate-dependent oxygenases are responsible for collagen modification by hydroxylating the proline (C-3 and C-4) and lysine residues (C-5), which both contribute to triple helical collagen stabilization (6). The 2OG-dependent oxygenases constitute a large family of enzymes with a highly

ABBREVIATIONS: BFA, brefeldin A; BSA, bovine serum albumin; Coll-I, collagen type I; Coll-IV, collagen type IV; CRISPR, clustered regularly interspaced short palindromic repeat; ECM, extracellular matrix; FBS, fetal bovine serum; Fn, fibronectin; HRP, horseradish peroxidase; Iono, ionomycin; PA, phosphatidic acid; PBS, phosphate-buffered saline; PS, phosphatidylserine; rJMJD6, recombinant JMJD6; scr, scrambled; siRNA, short interfering RNA; SPARC, secreted protein acidic and rich in cysteine; WB, Western blot

[1] Current affiliation: University of California, San Diego, La Jolla, CA, USA.

[2] Correspondence: Molecular Immunology Unit, Department of Experimental Oncology and Molecular Medicine, Fondazione IRCCS Istituto Nazionale dei Tumori, Via Amadeo 42 St., Milano, N/A 20133, Italy. E-mail: mariopaolo.colombo@istitutotumori.mi.it

doi: 10.1096/fj.201700377R

This article includes supplemental data. Please visit *http://www.fasebj.org* to obtain this information.

0892-6638/17/0031-5356 © FASEB

conserved structure and catalyze a wide range of oxidative reactions in microbes and plants. Two enzymatic activities, hydroxylation and demethylation of *N*-methylated groups within proteins and nucleic acids, have been identified in animals (7). The 2OG-dependent oxygenases belong to the JmjC subfamily (8), the members of which play a central role in the epigenetic regulation of gene expression during embryonic development and stem cell differentiation (9, 10). In tumors, their overexpression is associated with aggressive phenotype and cancer stem cell plasticity (11, 12).

JMJD6 is a member of the JmjC family. It was initially considered to be a transmembrane receptor specific for phosphatidylserine (PS) and necessary for the recognition of apoptotic cells by macrophages (13). Nevertheless, the presence of multiple nuclear localization signals in the protein sequence (14), its nuclear localization in transfected cells (15), its histone arginine demethylase activity (16), and the interaction with single-strand RNA (17), taken together, suggested a more complex role of JMJD6. Accordingly, it has been demonstrated more recently that JMJD6 targets a number of proteins, such as RNA-splicing-associated factors, histones, and p53 (18–20), through its lysyl hydroxylase activity while it modifies other proteins, such as ERα and HSP-70, through its demethylase activity (21, 22). In mice, JMJD6 knockout is lethal (23), supporting the idea that this enzyme plays a pivotal role during development. Moreover, JMJD6 overexpression in breast cancers is associated with poor prognosis (24), and its ectopic expression increases cancer cell line proliferation while its silencing reduces cell growth, motility, and invasion (24, 25). Through alternative nonenzymatic activities, JMJD6 modulates RNA splicing by interacting with the arginine–serine (RS) domains of SR and SR-like proteins (26) and controls adipocyte differentiation through transcriptional and post-transcriptional mechanisms (27).

In order to develop antibodies against molecules involved in stromal tissue modifications, we immunized *Sparc*-null mice, which display defective ECM organization and tissue remodeling, with wild-type tissues with the idea that these mice could immunologically recognize novel ECM structures generated in the presence of the matricellular protein SPARC. Using this approach, we isolated a mAb (P4E11) specific for JMJD6 and uncovered a new extracellular localization of JMJD6. Furthermore, we demonstrated that JMJD6 functionally interacts with collagen within the ECM and that this interaction can be inhibited by our novel P4E11 mAb.

MATERIALS AND METHODS

Reagents and antibodies

All reagents were a high-purified grade, and, if not otherwise specified, were purchased from Sigma-Aldrich (St. Louis, MO, USA). Purified recombinant JMJD6 (rJMJD6) protein (transcript variant 2, TP 308993) and the anti-DDK mAb recognizing a FLAG epitope on rJMJD6 protein were from OriGene Technologies (Rockville, MD, USA). Rat collagen type I (Coll-I) was purchased from BD Pharmingen (San Diego, CA, USA) (354236). Collagen type IV (Coll-IV) murine sarcoma (C0543), Fn from bovine plasma (F4759) and bovine serum albumin (BSA) were all purchased from Sigma-Aldrich. The following anti-JMJD6 Abs were used: mouse mAb: Santa Cruz Biotechnology (sc-28348) (Santa Cruz, CA, USA); rabbit polyclonal Abs: Sigma-Aldrich (P1495), Abcam (Cambridge, MA, USA) (ab64575), and Abnova (Taipei, Taiwan) (PAB2219). Anti-Coll-I Abs were from Sigma-Aldrich (mouse mAb C2456, rabbit polyclonal anti-human α2 chain, SAB 4500363), from Merck Millipore (Billerica, MA, USA) (rabbit polyclonal AB765P), and from Santa Cruz Biotechnology (mouse mAb recognizing mouse α2 chain, sc-393573). The rabbit polyclonal Abs anti-Coll-IV and anti-Fn were from Abcam (ab6586) and Sigma-Aldrich (F3648), respectively; mAbs anti-CD63 and anti-GAPDH were from Abcam (ab8219) and Sigma-Aldrich (G8795), respectively. The mouse mAb anti-Rab11 was from BD Transduction Laboratories (Lexington, KY, USA) (610657). Biotin rat anti-mouse CD45 (clone 30-F11) was from BD Pharmingen. Depending on the application, different purified IgG2a mAbs [553454 and W632, BD Pharmingen; HB-95, American Type Culture Collection(ATTC), Manassas, VA, USA] were used as isotypic control.

For use of anti-JMJD6 antibodies, because P4E11 mAb displayed reactivity in immunoprecipitation but not in Western blot (WB) analyses, we used the rabbit polyclonal anti-JMJD6 (Sigma-Aldrich) and the mAb (Santa Cruz Biotechnology) for WB staining. In particular, the polyclonal Ab has been used to test samples immunoprecipitated by P4E11 mAb and the mAb Santa Cruz Biotechnology for direct WB staining of cell samples and on lipid blots. For immunofluorescence analysis of JMJD6 cellular distribution, the rabbit polyclonal anti-JMJD6 (Sigma-Aldrich) was used in double staining together with mAbs recognizing endosomal markers (Rab11 and CD63).

Cell lines

The thioguanine-resistant 4T1 mouse breast carcinoma cell line (CRL-2539; ATCC) was from LGC-Promochem (Teddington, United Kingdom) (28, 29). The following human tumor cell lines were obtained from ATCC: MDA-MB-231 (HTB-26), MCF7 (HTB-22), SKBR3 (HTB-30), SKOV3 (HTB-77), MeWo (HTB-65), Jurkat (TIB-152), and U-937 (CRL-1953.2). The IGROV1 cell line was provided by the laboratory of S. Canevari (Fondazione IRCCS Istituto Nazionale dei Tumori); the A375M cell line (CRL 16199; ATCC) was provided by A. Carè (Istituto Superiore di Sanità, Rome, Italy); and the Mel 665.1 cell line was provided by A. Anichini (Fondazione IRCCS Istituto Nazionale dei Tumori). Cell lines were characterized by STR allele profile (D13S317, D16S539, D21S11, D5S818, D7S820, TH01, TPOX, and vWA) using the Geneprint 10 System kit (Promega, Madison, WI, USA).

Human and mouse cell lines were grown in RPMI 1640 medium and in DMEM, respectively, containing 1% glutamine and 10% fetal bovine serum (FBS) (PAA Laboratories, Colbe, Germany) in standard culture conditions (37°C and 5% CO_2). Cells were regularly checked for mycoplasma contamination by the MycoAlert detection kit (Lonza, Basel, Switzerland), with negative results.

Mice

BALB/c mice, aged 5 to 7 wk, were supplied by Charles River Laboratories (Wilmington, MA, USA). BALB/c $Sparc^{-/-}$ mice were developed in our institute as previously described (30). All animal treatments were authorized by the Institutional Ethics Committee for Animal Use at Fondazione Istituto di Ricovero e Cura a Carattere Scientifico (IRCCS) Istituto Nazionale dei Tumori.

Production of P4E11 mAb, and identification of target protein and recognized epitope

In order to obtain antibodies directed against components of the ECM, 2 $Sparc^{-/-}$ mice lacking the matricellular protein SPARC

were immunized twice with irradiated splenocytes deriving from SPARC-competent BALB/c mice. Hybridomas resulting from the fusion of splenic lymphocytes of one of them with NS0 myeloma cells were selected by culture in hypoxanthine–aminopterin–thymidine medium and their supernatants assayed by fluorescence-activated cell sorting analysis on permeabilized murine cells expressing or not expressing SPARC protein. Among these, P4E11 mAb (IgG2a) was chosen for a further characterization.

To identify the target protein, the mAb was tested by Thermo Fisher Scientific (Waltham, MA, USA) on a protein array (ProtoArray v.5.0; Thermo Fisher Scientfific) of 9400 human proteins. JMJD6, which resulted in one of the best statistically significant candidates, was validated by immunoprecipitation followed by WB analysis. The specific epitope on rJMJD6 recognized by mAb P4E11 was defined by differential mapping of rJMJD6 alone as well as by rJMJD6 + mAb P4E11 and rJMJD6 + mAb W632 (isotype control) at the Protein Microsequencing Facility (San Raffaele Scientific Institute, Milan, Italy).

P4E11 *in vivo* treatment

BALB/c mice, with each group consisting of 7 animals, were inoculated with 7×10^3 4T1 cells in the mammary fat, and the primary tumor growth was monitored for 4 wk. A group of mice was treated intraperitoneally with purified P4E11 (250 μg/inoculum) starting from the day before tumor injection twice a week for 4 wk. The control groups were treated with the same dose of unrelated antibody of the same isotype as P4E11 (IgG2a) or with saline. At the end of the treatment, animals were anesthetized and then humanely killed; the primary tumor was evaluated for size and removed for histochemical analysis. The approximate tumor volume was calculated by $r_{minor}^2 \times r_{major}$. Lungs were used for histochemical analysis and for evaluation of the metastatic disease in clonogenic assays, as described elsewhere (28). MDA-MB-231 cells (5×10^6) were inoculated in the mammary fat of immunodeficient SCID mice, and growth was monitored for 3 to 4 wk. IGROV1 cells (5×10^6) were inoculated intraperitoneally into immunodeficient nude mice, and the growth was monitored for about 3 wk. In both cases, the treatment groups (5 animals/group) included animals inoculated with P4E11 (same therapeutic regimen as above) and control animals inoculated with saline. The histologic analysis (Gomori reticulin and Masson trichrome staining) was conducted on solid primary tumors of MDA-MB-231 and on peritoneal adhering aggregates of IGROV1 cells.

Immunofluorescence on adherent cells

Cells seeded on glass slides were fixed with paraformaldehyde 2 to 4% for 20 min at room temperature and permeabilized with 0.1% Triton X-100 or 0.1% saponin as specified. Incubation with primary and secondary (Alexa Fluor, Molecular Probes, Eugene, OR, USA; Thermo Fisher Scientific) antibodies was performed as described (31). Samples were analyzed by confocal microscopy (Micro Radiance 2000; Bio-Rad, Hercules, CA, USA). Images were obtained using a ×60 oil immersion objective (512 × 512 pixels) by LaserSharp 2000 software (Carl Zeiss GmbH, Jena, Germany) and processed by Image-Pro Plus 7 software (Media Cybernetics, Rockville, MD, USA). Reported images represent a single central section on the *z* axis.

Histology and immunohistochemistry

Mouse and human tissues were fixed in 10% buffered formalin and embedded in paraffin. Histopathologic analysis was performed on 4 μm sections stained with hematoxylin and eosin, Gomori reticulin, and Masson trichrome. Human samples comprised formalin-fixed breast carcinoma specimens that were part of a study on ECM composition (32) carried out in our institute by E.T. under approval from the local ethics committee and in accordance with the Helsinki Declaration. Human melanoma and colon carcinoma were archival samples stored at the Human Pathology Section, University of Palermo, Palermo, Italy.

Immunohistochemistry was performed after antigen unmasking using Novocastra Epitope Retrieval Solutions pH 9 (Novocastra, Leica Biosystems, Wetzlar, Germany) using the PT Link system (Dako, Glostrup, Denmark) at 98°C for 30 min. Subsequently the sections were brought to room temperature and washed in phosphate-buffered saline (PBS). After neutralization of the endogenous peroxidase with 3% H_2O_2 and Fc blocking by a specific protein block, the samples were incubated for 1 h with the following primary antibodies: mouse mAb P4E11 (5 and 7 μg/ml); mouse mAb anti-JMJD6 (Santa Cruz Biotechnology) (4 μg/ml); mouse mAb anti-human Coll-I (clone 3G3; Acris, Herford, Germany) (5 μg/ml); and mouse mAb anti-human Coll-IV [clone 24.12.8 (PHM-12); Merck Millipore] (10 μg/ml), all at 4°C. Staining was revealed by the polymer detection kit method (Novolink Polymer Detection Systems, RE7280-K; Novocastra, Leica Biosystems) and AEC (3-amino-9-ethylcarbazole) substrate chromogen. The slides were counterstained with Harris hematoxylin (Novocastra, Leica Biosystems). Negative control stainings were performed by using mouse and rabbit immune sera instead of the primary antibodies. All the sections were analyzed under a DMD 108 optical microscope (Leica Microsystems, Buffalo Grove, IL, USA), and microphotographs were collected with the Axio Scope.A1 Axiocam 503 Color (Zeiss).

ELISA and JMJD6 peptide library

For ELISA tests, a library of 57 JMJD6 peptides, 14 aa long and overlapping each other for 7 aa, was synthesized by Primm (Milan, Italy). In each assay, the catcher protein, diluted in PBS at the proper concentration, was seeded in 96-wells plate and incubated ON at 4°C. After saturation with 1% BSA in PBS, specific incubations were carried out with soluble rJMJD6 or ECM proteins and then with secondary horseradish peroxidase (HRP)-conjugated antibodies (Zymed Laboratories, San Francisco, CA, USA; Thermo Fisher Scientific). All incubations were at room temperature, followed by 3 washings by PBS–0.1% Tween 20. The reaction was developed from tetramethylbenzidine (Sigma-Aldrich), stopped with 1 N H_2SO_4, and the plate read at 450 nm.

To test the capability of JMJD6 peptides to inhibit the interaction between Coll-I and rJMJD6, Coll-I was mixed with each peptide pool in 1000 times molar excess (the composition of each peptide pool is described in Supplemental Fig. S3*C*), and then incubated for 30 min at 37°C before seeding on plate ON at 4°C. Details of each assay are reported in the respective figure captions.

ECM extraction, and cell lysate and supernatant preparation

Overconfluent human cell line plates were treated with 20 mM NH_4OH in distilled water to eliminate the cell component. After washings, plates were treated with 1% SDS containing buffer and scratched to recover ECM proteins.

Cell lysates were obtained by treatment of the cells with lysis buffer containing 1% NP-40, 0.1% SDS, protease, and phosphatase inhibitors for 30 to 40 min on ice. The soluble fraction was recovered by centrifugation for 15 min at 13,000 rpm.

Culture supernatants were obtained from cells grown for 24 h at 37°C in medium without FBS and processed by differential

centrifugations (10 min at 1300 rpm, then 20 min at 2600 rpm). Protein content was evaluated by the bicinchoninic acid method (Thermo Fisher Scientific, Waltham, MA, USA) or alternatively by Bradford assay (Quick assay; Bio-Rad).

For other analyses, MeWo cell supernatant was also submitted to centrifugation (30 min at 10,000 *g*) and then to ultracentrifugation (2 h at 100,000 *g*) to obtain a soluble fraction (S_u) and a pellet (P_u). All the samples, before and after processing, were analyzed by WB, as previously described.

To test the factors which stimulate JMJD6 release, MeWo cells were treated for 17 h with medium without FBS containing brefeldin A (BFA) (5 μg/ml), ionomycin (Iono) (1 μg/ml), or DMSO (1:1000) as a control. At the end of the treatment, the supernatant was recovered and submitted to centrifugations and concentration as previously described for WB analysis.

SDS-PAGE, WB analysis, and immunoprecipitation

SDS-PAGE sample analysis, protein transfer, and immunoreactions as well as the immunoprecipitation experiments were carried out essentially as described elsewhere (31). For immunoprecipitation experiments, P4E11 and isotype control mAb were conjugated to epoxy-activated magnetic beads (Thermo Fisher Scientific). To test the interaction of Coll-I with rJMJD6, Coll-I (5 μg) was separated in SDS-PAGE under reducing conditions. After blotting, the membrane was stained red by Ponceau S, or saturated and incubated with rJMJD6, then with a primary anti-FLAG (DDK) mAb recognizing JMJD6 and subsequently with secondary HRP-conjugated anti-mouse antibodies before ECL. As a control, the anti-DDK reactivity was evaluated in the absence of rJMJD6. In parallel, the same amount of Coll-I was immunostained with anti-Coll-I antibodies with different specificity.

Silencing of JMJD6 expression by short interfering RNA transfection

MeWo cells (4.4×10^5 per sample) were grown for 24 h at 37°C, then transfected as described (31) with a mix of 2 short interfering RNA (siRNA) duplexes specific for JMJD6 (Trilancer-27 human siRNA; OriGene Technologies) or with unrelated scrambled (scr) negative control siRNA using Lipofectamine 2000 (Thermo Fisher Scientific). Seventy-two hours after removal of transfection reagents, cells were solubilized for immunoprecipitation with P4E11 mAb and WB.

Knockout of JMJD6 through clustered regularly interspaced short palindromic repeat/Cas9 technology

JMJD6 knockout MDA-MB-231 cells were obtained with clustered regularly interspaced short palindromic repeat (CRISPR)/Cas9 technology as described by Ran *et al.* (33). The human JMJD6 genomic sequence was analyzed with the CRISPR Design Tool (*http://tools.genome-engineering.org*) to identify potential genomic RNA targets, which were cloned in the pSpCas9(BB)-2A-GFP plasmid (ID 48138; a gift from F. Zhang, Addgene, Cambridge, MA, USA). MDA-MB-231 cells were then transfected with Lipofectamine 3000 reagent (Thermo Fisher Scientific) by using the pSpCas9(BB)-2A-GFP plasmid containing the 5′-GCTCTCGTAGTAGTTGTGCC-3′ genomic RNA (specific for JMJD6) or mock transfected with empty vector. After 48 h, green fluorescent protein–positive cells were sorted by fluorescence-activated cell sorting, and single cells were seeded in 96-well plates. Clones were then screened by WB and potential knockout clones further validated by sequencing.

Lipid blot immunoreaction

Nitrocellulose membrane with phospholipid spots (PIP strips, 100 pM; Echelon Biosciences, Salt Lake City, UT, USA) was saturated with 3% BSA in PBS, then incubated with rJMJD6 (0.5 μg/ml) in the same buffer. After 2-h incubation, the reaction proceeded by incubating with the primary anti-FLAG (DDK) or αJMJD6 mAb and secondary HRP-conjugated Abs, as described above for WB. As a control, a strip not incubated with rJMJD6 was stained with anti-FLAG and secondary anti-mouse Abs only.

Cell fractionation

Confluent MeWo cells, washed in PBS, were detached by scraping and lysed in hypotonic buffer HB-7S (5 mM Tris, 1 mM EDTA, 1 mM DTT, and 11% sucrose, pH 7.4), and processed by differential centrifugations as previously described (31) to obtain a final pellet considered the nuclear fraction and a supernatant, cleared of the crude membrane fraction, which constituted the cytosolic fraction.

Inhibition of cell adhesion by JMJD6 peptides

The assay was carried out to evaluate the adhesion of tumor cells (MDA-231, MeWo) to Coll-I substrate alone or mixed with JMJD6 or scr peptides in 100 times molar excess. Adhesion was evaluated after 2, 6, or 24 h incubation at 37°C. The adhesion to peptides alone in the absence of Coll-I was also tested. The percentage of cell adhesion at each time point was calculated considering the adhesion on Coll-I mixed with scr peptides as 100%.

Inhibition of fibrillogenesis by JMJD6 peptides

Rat Coll-I was diluted in 0.02 N acetic acid to obtain a soluble preparation. To induce the formation of insoluble fibrils, pH was increased to 7.4 by addition of Tris-HCl buffer, pH 8.3. After 30 min incubation at room temperature, the insoluble collagen was separated from the soluble one by centrifugation for 10 min at 13,000 rpm. The recovered supernatant and the dry pellet were analyzed by SDS-PAGE. Gels were stained by Simply Blue (GE Healthcare Life Sciences, Little Chalfont, United Kingdom). To evaluate whether JMJD6 peptides could interfere with Coll-I fibrillogenesis, each pool of peptides was mixed in 100× molar excess with Coll-I diluted in acetic acid, then Tris-HCl buffer, pH 8.3, was added. After incubation for 30 min at room temperature, samples were processed as described above. The percentage of soluble collagen in the supernatant was evaluated taking as 100% the amount of Coll-I present in the supernatant of Coll-I diluted in acetic acid.

Statistical analysis

One-way ANOVA and unpaired, 2-tailed Student's *t* test were used for statistical analysis.

RESULTS

JMJD6 is detectable in ECM *in vitro* and *in vivo*

To identify new targets within the tumor stroma that are potentially amenable for antibody-mediated treatments, we immunized *Sparc*-null mice with tissues derived from

syngenic wild-type BALB/c mice. Using this approach, we obtained a mAb, referred to as P4E11, which recognized an antigen expressed by permeabilized mouse and human tumor cell lines of different histotypes (data not shown). An array of over 9000 human proteins indicated JMJD6 as the most likely target of P4E11; this was confirmed by immunoprecipitation experiments with rJMJD6 protein and tumor cell lysates (**Fig. 1*A***). Specificity for JMJD6 was further confirmed by using MeWo cells silenced for JMJD6 expression and isogenic MDA-MB-231 cells either positive or negative for JMJD6 because of CRISPR/Cas9-mediated knockdown (Fig. 1*B*). In immunoprecipitation experiments, P4E11 recognized the monomeric form of JMJD6 (50 kDa) as well as high-molecular-weight oligomers (120–200 kDa). Because P4E11 also recognizes human JMJD6, we tested its reactivity in 22 cases of breast carcinoma, already characterized for ECM composition (32). As for the representative cases shown in **Fig. 2*A***, P4E11 mAb widely reacted with tumoral and stromal cellular elements, as well as with the ECM, as reported in Supplemental Table 1. High JMJD6 expression was observed in tumors (12 of 22 had the highest score of 3+, with 70 to 100% of cells stained), while the staining of ECM was less intense, with only 7 of 22 cases scored as 3+ and 11 of 22 samples classified as 1+. Most of these 1+ cases were characterized by a diffuse pattern of staining (8 of 11). The tissue immunolocalization of JMJD6 in the same 22 breast carcinomas stained with P4E11 mAb was confirmed using a commercial anti-JMJD6 mAb (Supplemental Fig. S1), which, however, displayed more intense and frequent nuclear staining. WB analysis, performed on the ECM extracted from plates after cell removal by hypotonic lysis (Fig. 2*B*), further supported ECM localization of JMJD6 in a panel of human tumor cell lines. These results demonstrated that P4E11 mAb recognizes JMJD6, which can also be detected in the extracellular milieu associated with the ECM.

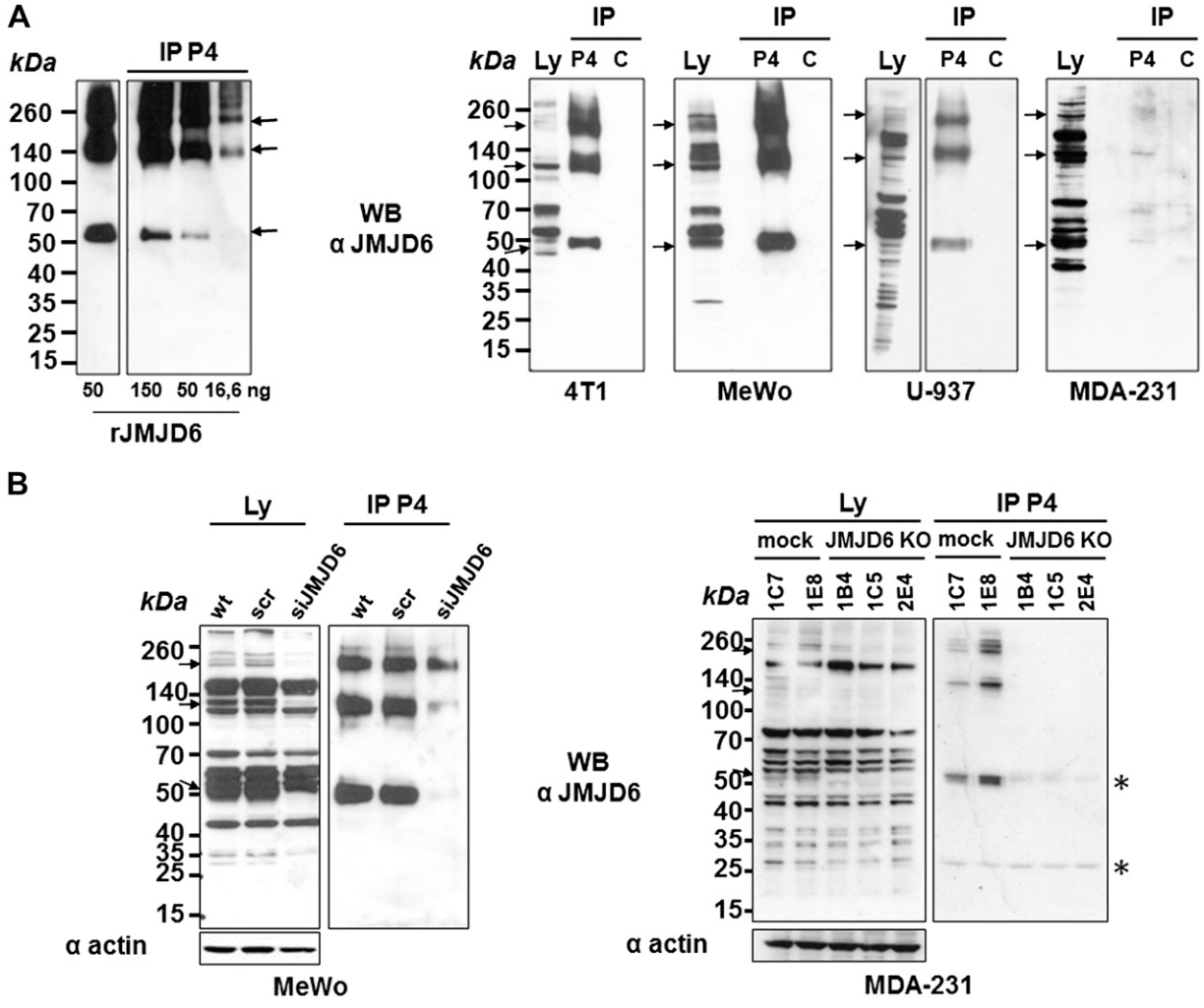

Figure 1. Specificity of P4E11 mAb for JMJD6. *A*) Validation of ProtoArray results by immunoprecipitation of recombinant JMJD6 (rJMJD6) (left) and tumor cell lysates (right) by P4E11 mAb (P4) and by control isotypic mAb (*C*). *B*) Immunoprecipitation of MeWo and MDA-231 cell lysates before and after inhibition of JMJD6 expression by siRNA (left) or CRISPR/Cas9 knockout (right), respectively. All WB analyses were carried out by polyclonal αJMJD6 Ab (Sigma-Aldrich). Arrows indicate JMJD6 monomeric and oligomeric forms of JMJD6 recognized by P4E11 mAb. Asterisks indicate immunoglobulin H and L chains from immunoprecipitating mAb.

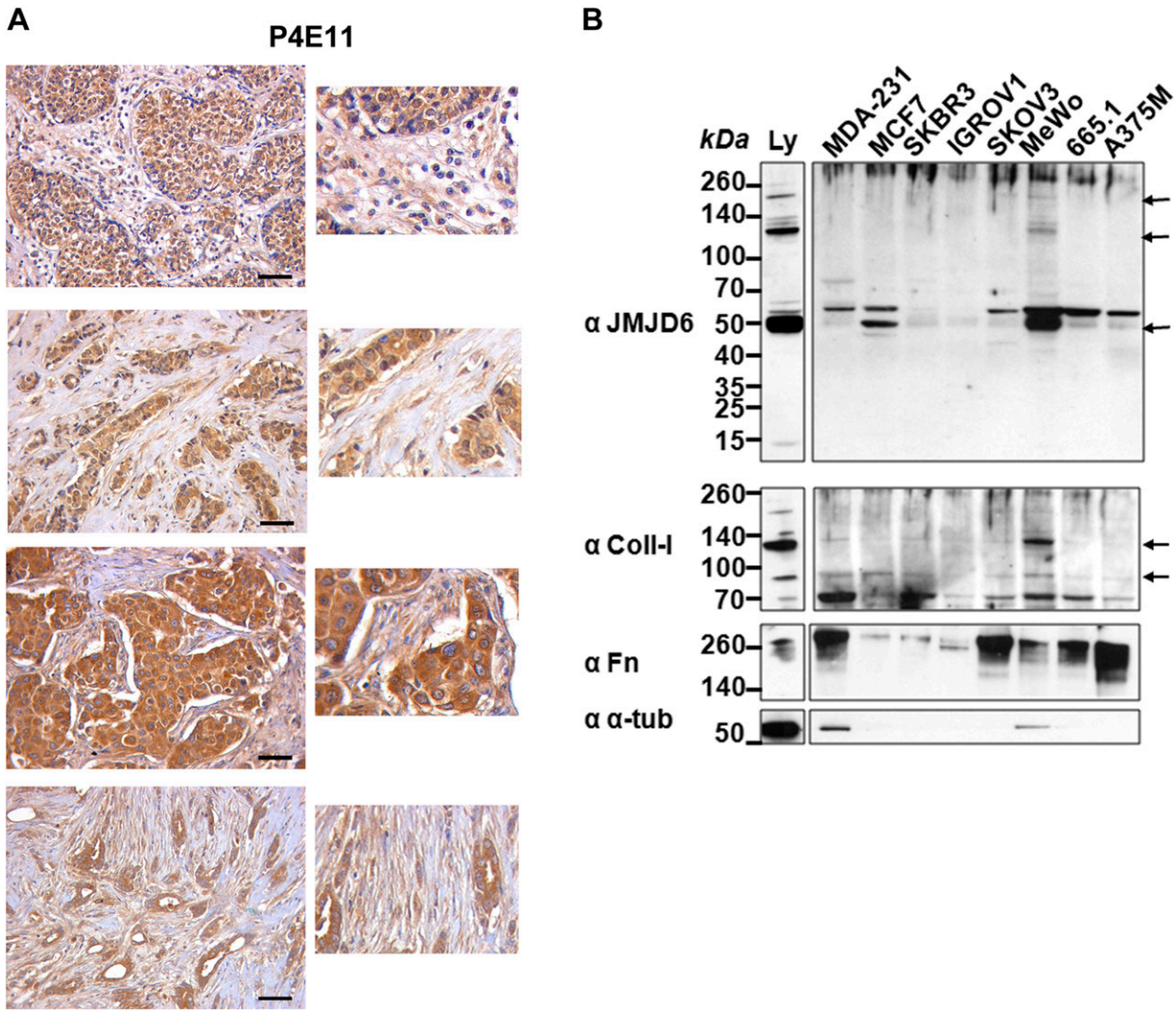

Figure 2. Reactivity of P4E11 mAb on ECM of human breast carcinoma and tumor cell lines. *A*) Immunohistochemical staining of 4 representative human breast carcinoma specimens as evaluated by P4E11 mAb. Scale bars, 100 μm. Magnification of extracted area, ×2. *B*) WB analysis of ECM proteins extracted from culture flasks of overconfluent human tumor cell lines compared to MeWo cell lysate (Ly). For each cell line, same volume of extracted 10× concentrated proteins was analyzed. Ly = 15 μg. Immunostaining of JMJD6 by anti-JMJD6 mAb (Santa Cruz Biotechnology). Staining of extracted ECM components, Coll-I and Fn, as positive control. α-Tubulin content monitored for possible presence of residual intracellular proteins. Arrows indicate monomeric and oligomeric forms of JMJD6, and mature and cleaved forms of Coll-I.

JMJD6 is secreted as soluble protein

To investigate whether JMJD6 could be secreted, the supernatants from the same panel of human tumor cells were tested by WB for the presence of JMJD6 and compared to their respective cell lysates. All cell lysates and supernatants contained both the 50-kDa monomer and the high-molecular-weight oligomers (120–200 kDa) of JMD6 (**Fig. 3*A***) as already observed in the immunoprecipitation experiments (Fig. 1).

The extracellular localization of JMJD6 was not predictable because it lacked the signal-peptide typical of secreted proteins. Nevertheless, even after ultracentrifugation, the supernatant (S_u) of MeWo cells contained both JMJD6 monomer and oligomers in soluble form (Fig. 3*B*), though a small fraction of JMJD6 was also detected in the CD63-positive pellet (P_u), which contained the exosome fraction. Soluble JMJD6 was also detected after ultracentrifugation in the supernatants of other human (Jurkat) and mouse (4T1) tumor cell lines (Supplemental Fig. S2*A*). In MeWo cells, neither the intracellular retention nor the block of secretion was induced by BFA, which instead inhibited Fn secretion that proceeds *via* Golgi vesicles (Fig. 3*C*). In contrast, treatment with the Ca^{2+} ionophore Iono induced a remarkable release of JMJD6 but negligible Fn secretion (Fig. 3*C*). Coll-I, which is normally secreted *via* Golgi vesicles, was not detectable in the supernatant of untreated or BFA-treated cells. Interestingly, Iono also induced the release of Coll-I. Taken together, these data show that cytoplasmic JMJD6 can be unconventionally secreted, as soluble protein, into the extracellular space, and that increased intracellular Ca^{2+} concentration stimulates its externalization.

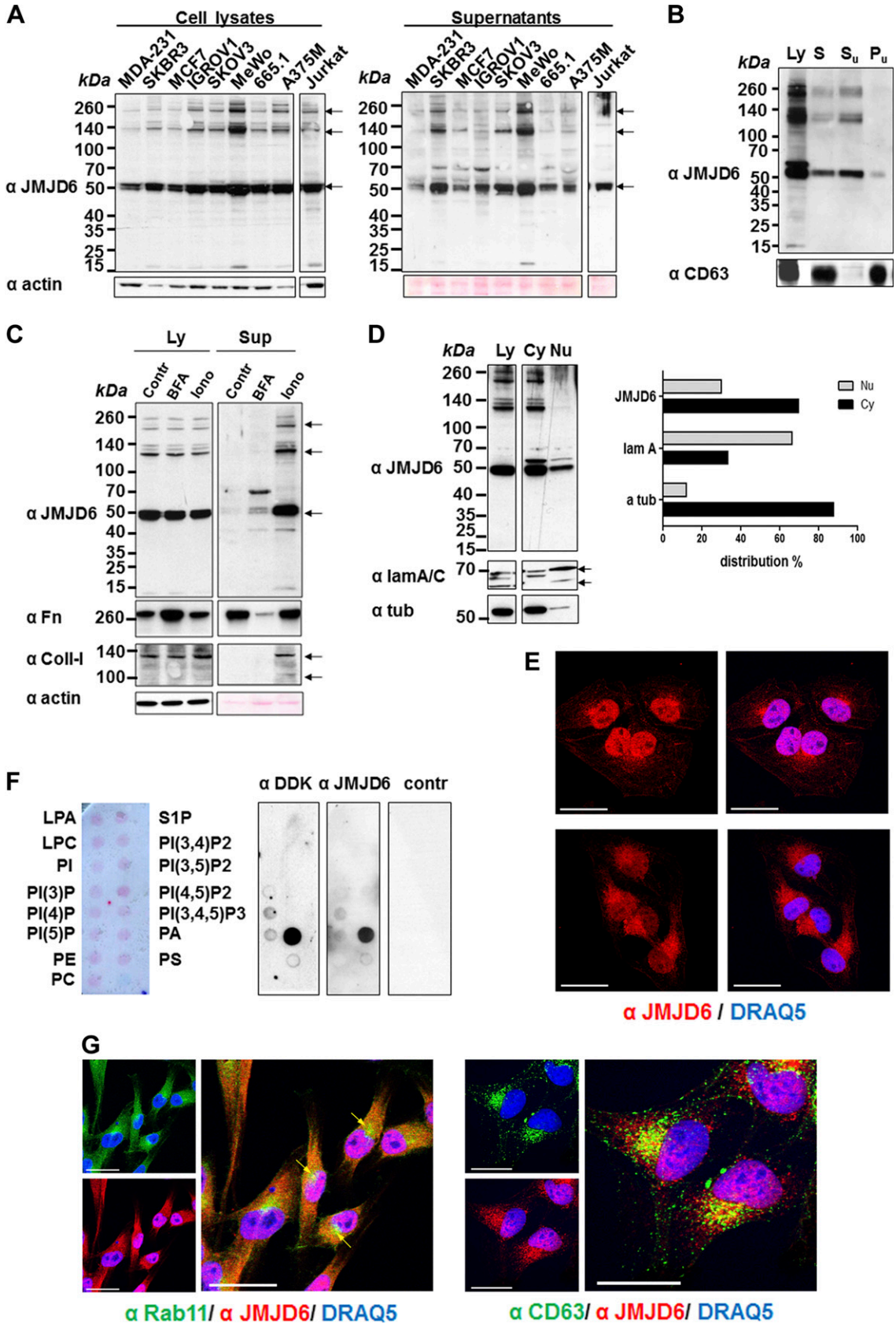

Figure 3. JMJD6 secretion, nucleo- or cytoplasmic localization, interaction with phospholipids, and association with intracellular vesicles. *A*) WB of cell lysates (left) and culture supernatants (right) of human tumor cell lines. Cell lysates = 15 μg; supernatants = 30 μg. Control for gel loading: actin content (lysates), red Ponceau S staining (supernatants). All WB analyses (*A–D*) were performed with anti-JMJD6 mAb (Santa Cruz Biotechnology). *B*) WB of MeWo cell lysates (Ly), of culture supernatants before

(*continued on next page*)

Cytoplasmic JMJD6 associates with intracellular vesicles

Biochemical fractionation and immunofluorescence staining demonstrated that JMJD6 is present in both the cytoplasm and the nuclei of MeWo cells (Fig. 3*D, E*). Some cytoplasmic proteins can be externalized through the interaction with lipids present in the membrane of intracellular vesicles. Protein sequence analysis of JMJD6 identified the presence of the K/RX(3-5)K/RXK/RK/R (aa 84–92) consensus sequence (34), which is functional for the binding to phospholipids (Supplemental Fig. S2*B*) and which differs from the sequence recently described in *Caenorhabditis elegans* as responsible for interaction with PS (35). Recombinant JMJD6 showed preferential interaction with phosphatidic acid (PA) and a much weaker interaction with PS and the inositol phosphates PI(4)P and PI(5)P (Fig. 3*F*). We subsequently stained MeWo cells with both anti-JMJD6 antibody and vesicle-specific markers and observed colocalization signals relative to JMJD6 and the recycling endosome marker Rab11, particularly around the microtubule organizing center (36), as well as between JMJD6 and CD63 (Fig. 3*G*). Rare foci of costaining were observed between JMJD6 and the early endosomal marker Rab5 (data not shown). These results confirm that JMJD6 is not only present in the cytoplasm as a soluble protein but also associates with intracellular vesicles marked by CD63 and Rab11, which might act as vehicles for JMJD6 externalization.

Interaction of rJMJD6 with ECM components

Having identified JMJD6 within the ECM, we tested whether recombinant rJMJD6 could directly bind with ECM components such as Coll-I and Fn seeded on plate. Serial dilutions (100, 10, and 1 nM) of flagged rJMJD6 showed a steady binding with rat Coll-I but a declining dose-dependent reactivity with Fn and no reactivity with BSA (**Fig. 4*A***). To further test the specificity and sensitivity of this interaction, plates were coated with serial dilutions of rat Coll-I, Coll-IV, Fn, and BSA, starting from 50 pM per well, and incubated with a fixed dose of rJMJD6 (10 nM). In these conditions, rJMJD6 stably binds to Coll-I diluted to 0.08 pM/well, whereas the binding to Coll-IV and Fn immediately dropped and was abolished at a concentration of 2 pM per well (Fig. 4*B*). Because of rJMJD6 interaction with purified rat and human Coll-I on the plate (data not shown), both collagens were analyzed by SDS-PAGE under reducing conditions to obtain the distinct α1 and α2 chains (Fig. 4*C*). After blotting on nitrocellulose membrane, anti-FLAG (DDK) mAb revealed that rJMJD6 selectively binds to the α1 chain of both rat and human Coll-I.

Identification of JMJD6 sequences mediating Coll-I interaction

A 14 aa JMJD6 peptide library covering the entire protein sequence was tested on a plate for recognition by the polyclonal and monoclonal anti-JMJD6 antibodies, which detect the intact recombinant JMJD6 protein (Supplemental Fig. S3*A*, inset). While the polyclonal Ab recognized peptides 52–54 (aa 358–385 of the protein) according to its specificity (immunizing peptide aa 363–381), no reactivity was detected by the commercial mAb, suggesting that it could recognize a conformational epitope, which is lost when the whole sequence is broken into fragments (Supplemental Fig. S3*A*). Also, the P4E11 mAb could recognize a conformational epitope. In fact, it is unable to react against any single peptide and even against the intact rJMJD6 that had previously been fixed on the plate. Nonetheless, the P4E11 mAb detects the JMJD6 soluble form.

We then tested whether any of these peptides could bind Coll-I. Peptides were seeded on a plate and incubated with rat Coll-I at the highest dose used in the assay reported in Fig. 4*B*. A polyclonal Ab against mouse Coll-I revealed Coll-I binding to multiple JMJD6 peptides, with 5 peaks of reactivity inside and 4 outside of the JmjC domain (**Fig. 5*A***). No Coll-I reactivity was detected on 2 scr peptides used as controls. In addition, the use of Fn instead of Coll-I in the same assay did not show any binding of Fn to JMJD6 peptides (Supplemental Fig. S3*B*). We subsequently tested whether the pools of peptides (Supplemental Fig. S3*C*), corresponding to the above-defined peaks of interaction, could inhibit the binding of the rJMJD6 to Coll-I. Although tested in a stronger molar excess (1000 times) than Coll-I, no peptide pool proved to inhibit rJMJD6 binding when Coll-I was preseeded on wells (Supplemental Fig. S3*D*). Conversely, when JMJD6 peptide pools were mixed at 37°C with Coll-I before their

(*S*) and after (S_u) ultracentrifugation, and of corresponding pellet (P_u). Ly = 15 μg. *S* = 30 μg and equivalent volume of S_u and P_u samples. Distribution of exosome marker evaluated by anti-CD63 mAb. *C*) WB of MeWo cell lysates and supernatants upon treatment with BFA or Iono compared to DMSO-treated control cells. Coll-I and Fn content used as positive control of conventionally secreted proteins. Actin expression (Ly) and red Ponceau S staining (Sup) were used as controls for gel loading. *D*) JMJD6 distribution in cytoplasmic (Cy) and nuclear (Nu) fractions of MeWo cells. Enrichment for cytoplasmic (α-tubulin) and nuclear (lamin A/C) markers evaluated in each fraction compared to cell lysate. Graphic illustrates relative distribution of JMJD6 (50-kDa band), lamin, and α-tubulin in nuclear and cytoplasmic fraction, as evaluated by densitometry analysis. *E*) Immunofluorescence staining and confocal microscopic analysis of MeWo cells by polyclonal anti-JMJD6 Ab (Sigma-Aldrich). Differential cell permeabilization by 0.1% Triton X-100 (top) and 0.1% saponin (bottom) to highlight nuclear or cytoplasmic JMJD6 localization, respectively. Nuclei are stained by DRAQ5. Single central section on *z* axis is reported. Scale bar, 20 μm. *F*) Interaction of rJMJD6 with phospholipids on nitrocellulose membrane as revealed by anti-FLAG (DDK) Ab or anti-JMJD6 mAb (Santa Cruz Biotechnology). Control membrane incubated with anti-FLAG mAb in absence of rJMJD6. *G*) Immunofluorescence staining and confocal analysis of MeWo cells permeabilized by 0.1% Triton X-100 (left) or 0.1% saponin (right) and double stained with anti-JMJD6 polyclonal Ab (Sigma-Aldrich) (red) and mAbs recognizing endosomal markers Rab11 and CD63 (green). Nuclei are stained by DRAQ5. Single central section on *z*-axis is reported. Scale bars, 20 μm. Yellow arrows indicate Rab11/JMJD6 costaining near microtubule organizing center.

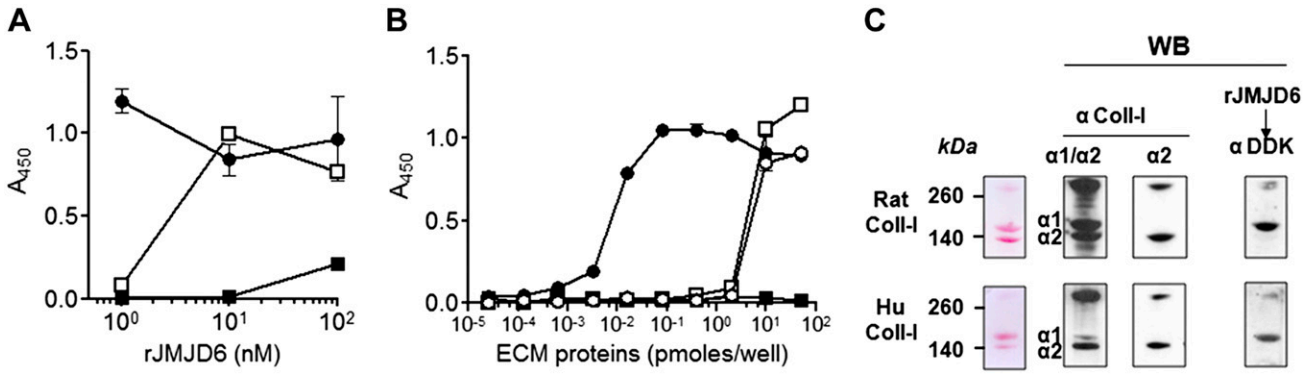

Figure 4. JMJD6 binding to Coll-I. *A*) ELISA on ECM proteins showing binding of rJMJD6 (100, 10, 1 nM) to Coll-I (solid circles) and Fn (open squares) in plate (50 pM/well) revealed by anti-FLAG (DDK) mAb. BSA (solid squares) was negative control. *B*) ELISA showing binding of 10 nM rJMJD6 to serial dilutions of Coll-I (solid circles), Coll-IV (open circles), and Fn (open squares) seeded in plate starting from 50 pM per well. Interaction was revealed by anti-FLAG (DDK) mAb. BSA (solid squares) was used as negative control. *C*) Interaction of rJMJD6 with blotted rat and human Coll-I (5 μg/lane), as revealed by anti-FLAG (DDK) mAb (right). At left, collagen staining by red Ponceau S. In middle, staining of Coll-I α1 and α2 chains or of α2 chain alone by specific anti-Coll-I antibodies.

seeding on a plate, both inhibition and enhancement of rJMJD6 binding were observed, depending on the peptide pools tested (Fig. 5*B*). Pools containing sequences belonging to the JmjC domain displayed limited or no inhibition of rJMJD6 binding to Coll-I, whereas those included into the external regions of the protein, either N- or C-terminal, enhanced the interaction between rJMJD6 and Coll-I up to 2- to 3-fold (Fig. 5*B*). As a control, scr peptide pool mixed to Coll-I did not modify the binding of rJMJD6 to Coll-I. These results were consistent in 4 distinct experiments for all peptide pools except for pool F, the activity of which varied widely among the experiments.

To further investigate the interaction between specific regions of JMJD6 protein and Coll-I, we performed an *in vitro* fibrillogenesis experiment. Using this assay, we tested whether pools of JMJD6 peptides (A, B, E, and I) mixed to Coll-I could interfere with fibrillogenesis. Compared to the Coll-I/scr peptide mix showing decreased soluble collagen from 100 to 12% at physiologic pH, the mix containing the peptide pool I—and, less efficiently, pool A—maintained the collagen soluble at 46.87 and 26.4%, respectively, thus antagonizing fibril formation (Fig. 5*C*).

In summary, we demonstrated that a mechanical interaction between JMJD6 and Coll-I takes place *in vitro* and that this interaction can modify Coll-I behavior. This suggests that the binding of JMJD6 peptides to Coll-I during fibrillogenesis could influence the interaction with other proteins present in the ECM. To test this hypothesis, we investigated the effects of JMJD6 peptides on the interaction between Coll-I and Fn.

JMJD6 peptides modulate Coll-I/Fn interaction and collagen-mediated cell adhesion

Fn interacts with Coll-I *in vivo* and contributes to ECM stabilization. We tested whether the binding of Fn to Coll-I could be inhibited by any of JMJD6 peptide pools premixed with Coll-I at 37°C. Pool C and especially pool G inhibited the Fn binding to Coll-I (26.8% and 81.8%, respectively) when used at 1000 times excess (Fig. 5*D*), thus confirming our hypothesis.

Both Coll-I and Fn contribute to cell-substrate adhesion through integrin-mediated recognition of specific sequences. We hypothesized that JMJD6 peptides mixed with Coll-I could modulate cell adhesion interfering with cell–collagen interaction. In agreement with our notion, the JMJD6 peptides corresponding to pools A, B, H, I, and F reduced the short-term (2 h) adhesion of the breast carcinoma cell line MDA-MB-231 to the Coll-I substrate from 100% of control scr peptide pool to 61.8, 51.3, 64.5, 46.9, and 56.8%, respectively (Fig. 5*E*). Moreover, the inhibition mediated by peptide pools A, B, and I was persistent all along the observation time of 24 h (Fig. 5*F*). The seeding of the sole peptide pools, in the absence of Coll-I, was insufficient to block MDA-MB-231 cell adhesion (Supplemental Fig. S3*E*). Comparable results were obtained investigating the short-term adhesion of the human melanoma cell line MeWo (Supplemental Fig. S3*F*). These results indicate that specific JMJD6 peptides impair both collagen binding to Fn and cell adhesion.

P4E11 mAb binding to rJMJD6 is mutually exclusive from Coll-I

In light of the above-reported results, we reevaluated the P4E11 mAb, which displayed reactivity in immunoprecipitation but not in WB analyses. Accordingly, the epitope recognized on rJMJD6 proved to be sensitive to heat denaturation (Supplemental Fig. S4*A*). Moreover, binding of P4E11 to soluble rJMJD6 was impaired when another anti-JMJD6 antibody engaged the recombinant protein first (**Fig. 6*A***, column 2). However, the primary interaction of P4E11 with rJMJD6 left the JMJD6 recognition unchanged by this Ab (Fig. 6*A*, column 1). This suggests that there is no competition for the same epitope but rather that P4E11 recognizes a distinct epitope on JMJD6, the conformation of which could be modified through the interaction with

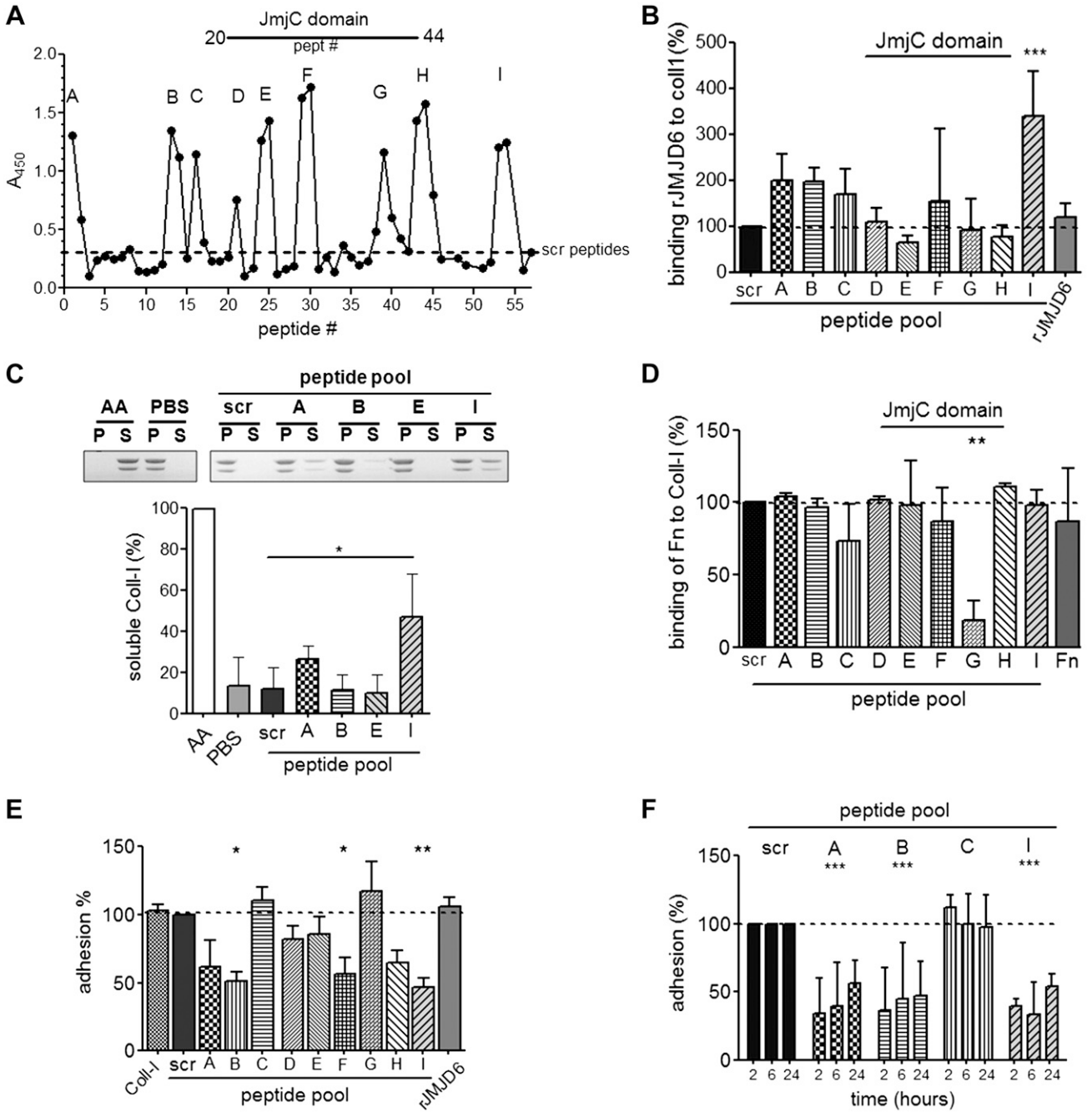

Figure 5. Interaction of Coll-I with JMJD6 peptides and peptide-induced modulation of collagen properties and cell adhesion. *A*) ELISA showing Coll-I binding to JMJD6 peptides seeded in plate (1 μg/well) and incubated with rat Coll-I (50 pM/well) and then with anti-Coll-I antibody (solid line). Binding of Coll-I on pool of 2 scr peptides (dashed line) as control. *B*) Effect of JMJD6 peptides on binding of rJMJD6 to rat Coll-I. Mix of rat Coll-I (0.2 pM/well) and JMJD6 peptide pools (1000 times molar excess) was preincubated for 30 min at 37°C before seeding in plate. Binding of rJMJD6 (50 pM/well) to Coll-I was revealed by anti-FLAG (DDK) mAb. Percentage of collagen binding was evaluated taking as 100% binding of rJMJD6 to mix Coll-I/scr peptides (means ± SD, $n = 4$ separate experiments; 1-way ANOVA; $P < 0.0001$). Peptide pool composition shown in Supplemental Fig. S3*C*. *C*) *In vitro* fibrillogenesis assay of rat Coll-I in presence of JMJD6 peptides was carried out as described in Materials and Methods. Soluble and insoluble fibrillar Coll-I were separated by SDS-PAGE and respective amounts evaluated by densitometry analysis after gel staining. Amount of soluble Coll-I was calculated taking as 100% solubility in acetic acid (means ± SD, $n = 3$ separate experiments; 1-way ANOVA; $P = 0.0169$). *D*) Inhibition of interaction between Coll-I and Fn by JMJD6 peptide pools. Rat Coll-I (0.2 pM/well) premixed 30 min at 37°C with peptide pools (1000 times molar excess) was seeded in plate. Interaction with Fn (100 nM) detected by incubation with anti-Fn antibody and expressed as binding percentage with respect to Coll-I mixed to scr peptides (means ± SD, $n = 2$ separate experiments; 1-way ANOVA; $P = 0.0215$). *E*) Short-term (2 h) adhesion assay of MDA-MB-231 cells on Coll-I (10 μg/well) premixed in batch with JMJD6 peptide pools (100 times molar excess). Percentage of adhesion evaluated taking as 100% adhesion value on Coll-I mixed with scr peptides (means ± SD, $n = 2$ separate experiments; 1-way ANOVA; $P = 0.0006$). *F*) Kinetics of adhesion of MDA-231 cells on Coll-I premixed with 100 times molar excess of JMJD6 peptide pools A–C and I, and scr peptides, tested at 2, 6, and 24 h. Adhesion was evaluated taking as 100% adhesion on Coll-I mixed with scr peptides (means ± SD, $n = 3$ separate experiments; 1-way ANOVA; $P < 0.0001$).

other Abs or other proteins. Indeed, P4E11 was unable to recognize rJMJD6 already bound to Coll-I, while the majority of commercial anti-JMJD6 Abs tested and the anti-FLAG (DDK) mAb correctly bound JMJD6, regardless of its interaction with Coll-I (Fig. 6*B*).

The mutual interference between P4E11 and Coll-I for binding to rJMJD6 was confirmed in an *ad hoc* assay where P4E11 seeded on a plate interacted with JMJD6 before, but not after, addition of Coll-I (Fig. 6*C*, left). This interference was specific for P4E11 because the polyclonal αJMJD6 Ab (Sigma-Aldrich) was unable to compete with Coll-I for its binding with JMJD6 under the same experimental conditions (Fig. 6*C*, right). In both cases, JMJD6 was equally recognized by the polyclonal αJMJD6 (Fig. 6*C*, left) or anti-FLAG (DDK) mAbs (Fig. 6*C*, right) either in the presence or in the absence of Coll-I. These results demonstrated that the P4E11 mAb recognizes on JMJD6 a conformational epitope deputed for interaction with collagen and that the binding of P4E11 or Coll-I to JMJD6 is mutually exclusive. This conclusion was supported by immunohistochemistry performed in 2 representative cases of breast carcinoma where the staining of extracellular JMJD6 by P4E11 mAb

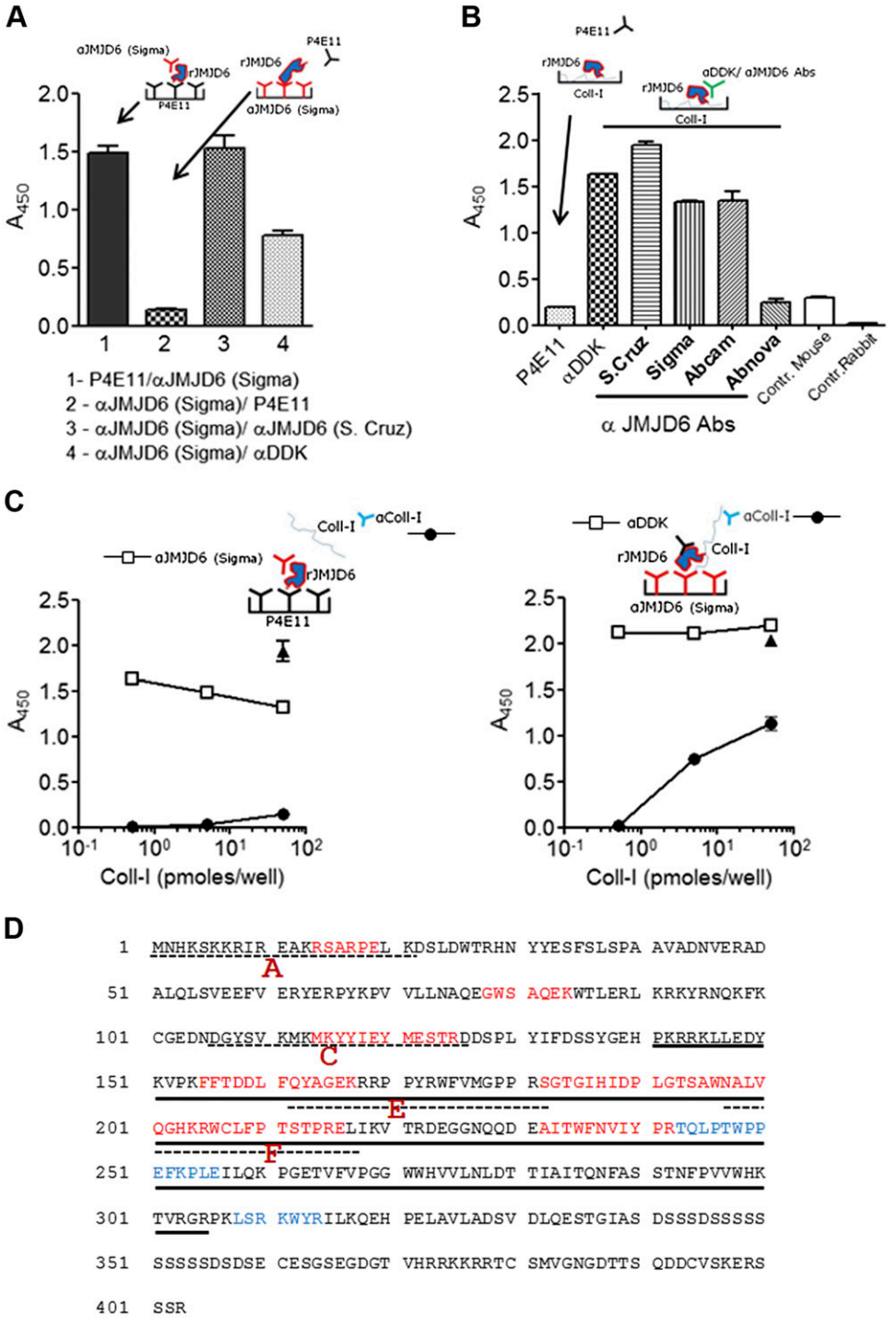

Figure 6. P4E11 mAb recognizes conformational epitope on rJMJD6 excluding interaction with Coll-I. *A*) ELISA for soluble rJMJD6 double recognition by anti-JMJD6 Abs. Catcher Abs [P4E11 mAb (P4) or polyclonal rabbit (Rb) (Sigma-Aldrich)] were seeded in plate; interaction was revealed by incubation with polyclonal Rb αJMJD6 or by mAbs [P4E11, αJMJD6 mAb (Santa Cruz Biotechnology), and anti-FLAG (DDK)], respectively. *B*) Binding of rJMJD6 (10 nM) to Coll-I in plate (50 pM/well) as detected by P4E11, anti-FLAG (DDK), and 4 commercial rabbit polyclonal anti-JMJD6 Abs or secondary Abs alone as control. *C*) P4E11 mAb (left) or polyclonal Rb αJMJD6 Ab (Sigma-Aldrich) (right) seeded on plate (1 μg/well) were incubated with rJMJD6 (50 pM/well). Capability of captured rJMJD6 to bind rat Coll-I (50, 5, and 0.5 pM/well) was verified by anti-Coll-I polyclonal (left) or monoclonal (right) Abs (solid circles), while bound rJMJD6 in presence (open square) or in absence (solid triangle) of Coll-I was monitored by using polyclonal anti-JMJD6 Ab (Sigma-Aldrich) (left) or anti-FLAG (DDK) mAb (right), respectively. One representative experiment of 2 having superimposable results. *D*) P4E11 epitope mapping on JMJD6 protein sequence. Red indicates amino acid sequences specifically protected from enzymatic digestion by incubation with P4E11 mAb; blue, amino acid stretches bound by both P4E11 and isotypic control antibody. Indicated are amino acid sequences corresponding to JMJD6 peptide pools that bind Coll-I (pools A, C, E, and F) and are at least partially superimposable to P4E11 epitope (solid line). JmjC domain is underlined.

was inversely correlated with the content of Coll-I (Supplemental Fig. S4*B*, rows 1 and 2, respectively). The same inverse correlation was also seen in cases of colon carcinoma and melanoma representative of high and low expression of JMJD6 detected by P4E11 mAb (Supplemental Fig. S4*B*, rows 3 and 4, respectively). The staining for Coll-IV did not correlate with the presence of JMJD6 (Supplemental Fig. S4*B*, right lane).

The mapping of the JMJD6 epitope recognized by P4E11 confirmed its conformational nature. The epitope was identified through the sequencing of amino acid stretches protected from protease digestion due to P4E11-JMJD6 interaction (Fig. 6*D*). Three stretches were located in the N-terminal region. Their sequences corresponded to aa 14–19 (included in peptides 1–2, pool A), aa 78–84 (peptides 11–12), and aa 114–125 (included in peptides 16–17, pool C). The other 3 sequences were identified in the JmjC domain and corresponded to aa 155–167 (peptides 22–24, with 24 being included in pool E), aa 182–216 (peptides 26–30, with 29–30 being in pool F), and aa 225–252 (peptides 33–35). JMJD6 peptides of pools A, C, E, and F were involved in Coll-I interaction (Fig. 5*A*), and peptides 26 to 27 contained 2 aa, 187 (H/histidine) and 189 (D/aspartic acid), responsible for Fe^{2+} binding. These results demonstrate that the P4E11 mAb may have a dual function: it can block JMJD6 binding to Coll-I, and at the same time it could inhibit JMJD6 enzymatic activity through occupancy of the JmjC domain.

In vivo biologic activity of anti-JMJD6 mAb P4E11

It has been recently reported that overexpression of JMJD6 is associated with poor prognosis in human breast cancer (24) and other tumor histotypes (37). We tested whether the P4E11 mAb could exert any relevant biologic effect *in vivo* using the 4T1 mouse model of high-grade metastatic breast cancer. Intramammary fat pad injection of 4T1 cells gave rise to primary tumors of comparable size in 2 groups of mice treated with either P4E11 mAb or an isotype-matched control mAb (**Fig. 7*A***). Strikingly, the frequency of metastases in the lung parenchyma was markedly reduced in P4E11 mAb-treated mice compared to mice treated with the isotype control (Fig. 7*B*). Histology of primary tumors from P4E11 mAb–treated mice revealed abundant leukocyte infiltration detected by $CD45^+$ cell staining (Fig. 7*C, D*); disarranged stromal fibrovascular septa with consistently reduced collagen content, as revealed by direct collagen staining and quantification (Fig. 7*C, E*); Masson trichrome blue staining (Fig. 7*C*); and less frequent collagen fiber intersections, according to Gomori reticulin staining of reticular collagen (Fig. 7*C*). These results indicate that P4E11-mediated targeting of JMJD6 significantly reduced the metastatic burden, possibly interfering with the cell-to-matrix interaction, and also exerted antifibrotic activity, most likely through the modulation of collagen content and distribution.

The interference in the JMJD6–collagen interaction mediated by P4E11 mAb was confirmed in 2 models of human tumor xenografts: MDA-MB-231 breast carcinoma cells grown in the subcutaneous fat pad (Fig. 7*F*), and IGROV1 ovary carcinoma cells forming tumor masses adherent to the peritoneum (Fig. 7*G*). In both cases, a reduced collagen content and matrix simplification were observed in tumors from P4E11-treated mice (Fig. 7*F, G*).

DISCUSSION

The Fe^{2+}- and 2OG-dependent oxygenase family includes enzymes with different functions, including regulation of gene expression through epigenetic modifications and stabilization of collagen chains during collagen synthesis (6). JMJD6, a JmjC domain–containing Fe^{2+}- and 2-oxoglutarate-dependent dioxygenase with histone demethylase and lysyl hydroxylase activity, has been recently associated to tumor progression (38). Here we demonstrate that JMJD6 can be part of the ECM milieu, where it binds to Coll-I (α1 chain), and that the Ab-mediated inhibition of such interaction has antimetastatic and antifibrotic effects.

To our knowledge, this is the first evidence of JMJD6 expression not confined to the nucleus and cytoplasm, but present also in the extracellular space as a secreted soluble protein or associated with the ECM. As for other cytoplasmic or nuclear proteins lacking the signal peptide (39), the release of JMJD6 occurs through an unconventional mechanism that, insensitive to BFA inhibition, allows its passage from the cytoplasm to the extracellular milieu. This is likely to occur through the interaction with membrane phospholipids, such as PA and PS, located at the surface of intracellular vesicles and plasma membrane (Fig. 3*F, G*). PS has been suggested to be the ligand of JMJD6 (13). It is enriched in the luminal leaflet of endoplasmic reticulum and Golgi complex, and it is also expressed at the cytosolic surface of the endosome/endocytic recycling compartment (40). Here, PS regulates protein sorting in the exocytic vesicles (41). In this context, PS could interact with cytoplasmic JMJD6, favoring its externalization. Also, PA regulates exocytosis in several cell types, and its production by phospholipase D through phosphatidylcholine hydrolysis is stimulated by Iono-induced Ca^{2+} fluxes (42), which, we show, enhance JMJD6 secretion. PA is present in vesicles such as Rab11-positive recycling endosomes, late endosomes, and CD63-positive exosomes (43), all of which costained with the anti-JMJD6 polyclonal Ab. Therefore, exosomes might represent an additional way to release JMJD6, as suggested by its presence in the pellet obtained by ultracentrifugation of MeWo and Jurkat cells' supernatant (Fig. 3*B* and Supplemental Fig. S2*A*).

We demonstrate that JMJD6 binds to Coll-I, and we identified the specific sequences that, on JMJD6, are responsible for this interaction (Figs. 4 and 5*A*).The possibility that JMJD6 could enzymatically modify Coll-I is unlikely. In fact, the products of JMJD6 lysyl hydroxylase activity display C-5 hydroxylysine residues with 5S stereochemistry, while collagen lysyl hydroxylases give lysyl hydroxylated products with 5R stereochemistry (44). On the basis of our data, we hypothesize that some amino acid sequences present in the JMJD6 peptides and interacting

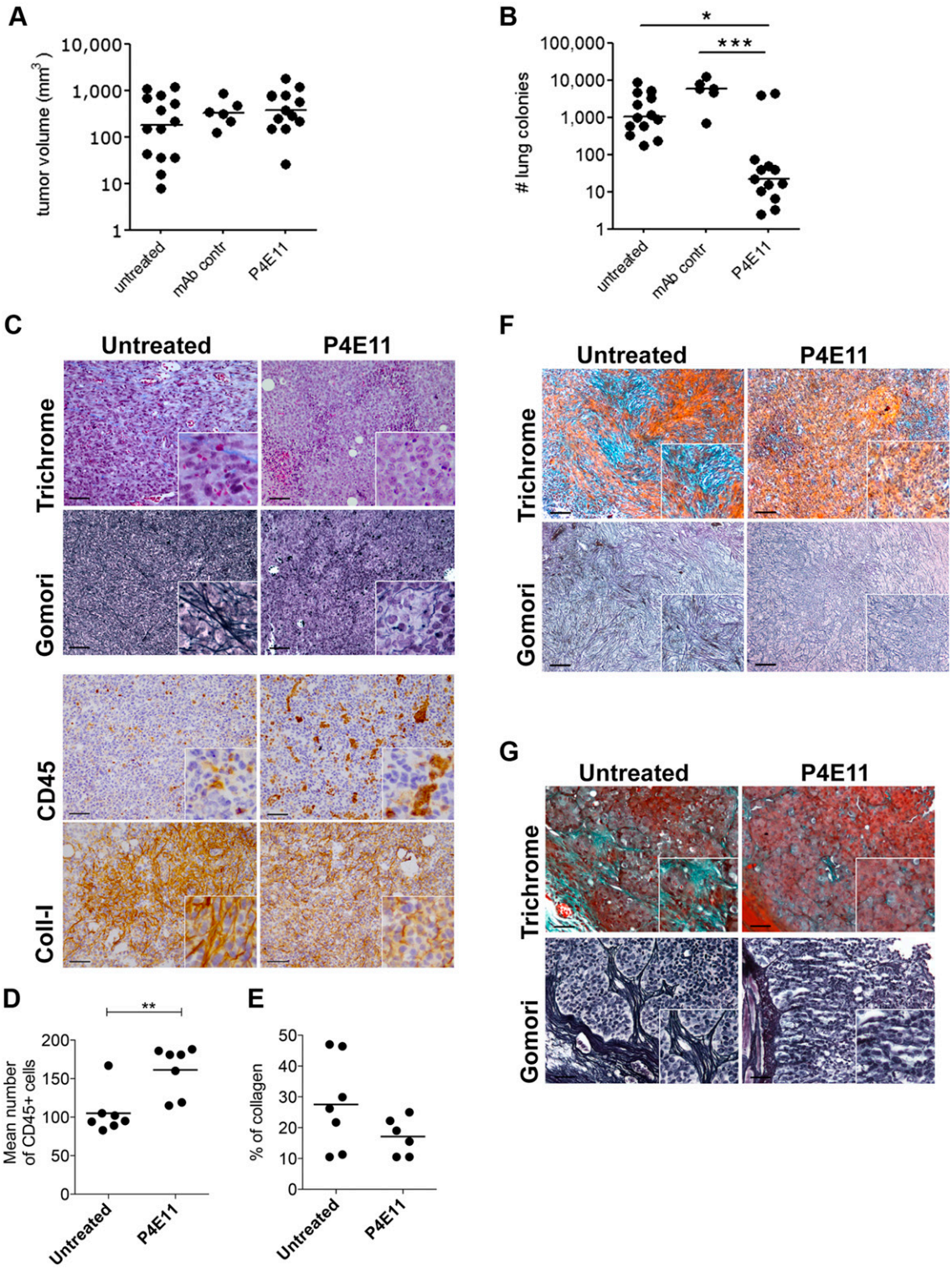

Figure 7. Antimetastatic and antifibrotic activity *in vivo* of anti-JMJD6 P4E11 mAb. *A*) Primary tumor volumes in mice inoculated with 4T1 cells (7×10^3) and treated with P4E11 mAb or with control mAb of same isotype or physiologic solution (untreated). Data derive from 2 separate experiments of 7 animals each. Treatment with control mAb was performed only in 1 of 2 experiments. Differences were evaluated by Student's *t* test and were found to be not statistically significant. Median value is indicated. *B*) Lung metastatic spread of 4T1 cells in same mice evaluated by clonogenic assay. Difference in lung colonies evaluated by 2-tailed Student's *t* test: untreated *vs.* P4E11, $P = 0.0457$; mAb control *vs.* P4E11, $P = 0.0003$. *C*) Masson trichrome staining, Gomori reticulin staining, lymphoid infiltrate (CD45 staining), and collagen content of representative sample of 4T1 primary tumor from mice treated with physiologic solution (untreated) or P4E11 mAb. Scale bars, 100 μm. *D*) Quantitative evaluation of CD45-positive cells and collagen content (*E*) in 7 samples of 4T1 tumor treated or not with P4E11 mAb. *F*) Masson trichrome and Gomori reticulin staining of representative sample of MDA-231 primary tumor from SCID mice treated with physiologic solution (untreated) or with P4E11 mAb. Scale bars, 100 μm. *G*) Masson trichrome and Gomori reticulin staining of representative sample of peritoneal fragment from nude mice injected with IGROV1 cells and treated with physiologic solution (untreated) or with P4E11 mAb. Scale bars, 100 μm. Magnification of extracted areas, ×1.5 (*F*, *G*), ×3 (*C*).

with Coll-I interfere with collagen fibrillogenesis and most likely modulate the interaction of Coll-I with other ECM proteins, such as Fn (Fig. 3 and Supplemental Fig. S5). Fn/Coll-I interaction involves specific sequences at the N terminal of Fn (45) and a binding region on the α1 chain of Coll-I (46). Moreover, collagen fibril formation is strictly connected with Fn assembly under the cellular control exerted by interaction with integrins (47). The complex network of interactions between collagen, Fn, integrins, and other collagen receptors modulate cell adhesion and migration. We found that some JMJD6 peptides are able to reduce cell adhesion to Coll-I. Notably, the same peptide pools (particularly I and A) capable of reducing cell adhesion have also been shown to increase the binding of rJMJD6 to Coll-I and to modulate collagen fibrillogenesis (Fig. 5*B, C*, respectively). *In vivo*, reduced cell adhesion caused by JMJD6 might result in early metastasis and this effect is counteracted by P4E11 mAb, as shown in the 4T1 model of spontaneous metastasis. Moreover, P4E11 showed a marked antifibrotic activity at the primary site (Fig. 7*C, E*). Similar to normal tissues, fibrosis also arises in tumors as a result of deregulated and uncontrolled ECM synthesis, particularly of collagens (48). In the primary tumor, fibrosis contributes to tumor progression and enhances metastatic spread (49). We hypothesize that the P4E11 mAb inhibits the binding of JMJD6 to Coll-I at the extracellular level immediately after secretion, which for both JMJD6 and Coll-I is induced by Iono treatment, and before other profibrotic extracellular modifications of collagen can take place (50). Moreover, because P4E11 mAb does not bind to conformationally altered rJMJD6 nor its peptides, one possibility is that the interaction of the antibody with the protein could block ECM matrix metalloproteinase–mediated JMJD6 digestion. Accordingly, low-molecular-weight polypeptides recognized by polyclonal anti-JMJD6 Ab are present in the supernatant of 4T1 cells (Supplemental Fig. S2*A*), and we have preliminary data suggesting that rJMJD6 is susceptible to matrix metalloproteinase enzymatic activity *in vitro*.

In line with other studies where the JMJD6 molecular interactions and not its enzymatic activity mediate the protein function (26, 27), our data reveal new biologic properties of JMJD6 and of JMJD6-derived peptides apparently independent of JmjC-domain activity. However, the peculiar characteristics of P4E11 mAb in recognizing a conformational target epitope, which also includes amino acid sequences of the JmjC domain, do not exclude the notion that *in vivo*, a wide range of activities might be modulated by the antibody, including the JMJD6 enzymatic activity itself. For all these reasons, the anti-JMJD6 mAb P4E11 may represent a new opportunity to target fibrotic and tumor diseases. Fj

ACKNOWLEDGMENTS

The authors thank C. Melani (Fondazione IRCCS Istituto Nazionale dei Tumori) for initial characterization of P4E11 mAb; A. Andolfo and D. Drago (Protein Microsequencing Facility, San Raffaele Scientific Institute) for P4E11 epitope mapping; and I. Facetti (Fondazione IRCCS Istituto Nazionale dei Tumori) for technical support. The authors also thank the Associazione Italiana per la Ricerca sul Cancro for financial support (Grant IG 10137 to M.P.C.). The authors declare no conflicts of interest.

AUTHOR CONTRIBUTIONS

S. Miotti and M. P. Colombo designed the research; S. Miotti, A. Gulino, R. Ferri, M. Parenza, A. Chronowska, D. Lecis, and S. Sangaletti performed research; S. Miotti, A. Chronowska, C. Tripodo, and M. P. Colombo analyzed data; E. Tagliabue contributed new reagents; and S. Miotti, D. Lecis, and M. P. Colombo wrote the article.

REFERENCES

1. Mouw, J. K., Ou, G., and Weaver, V. M. (2014) Extracellular matrix assembly: a multiscale deconstruction. *Nat. Rev. Mol. Cell Biol.* **15**, 771–785
2. Bradshaw, A. D. (2009) The role of SPARC in extracellular matrix assembly. *J. Cell Commun. Signal.* **3**, 239–246
3. Csiszar, K. (2001) Lysyl oxidases: a novel multifunctional amine oxidase family. *Prog. Nucleic Acid Res. Mol. Biol.* **70**, 1–32
4. Levental, K. R., Yu, H., Kass, L., Lakins, J. N., Egeblad, M., Erler, J. T., Fong, S. F., Csiszar, K., Giaccia, A., Weninger, W., Yamauchi, M., Gasser, D. L., and Weaver, V. M. (2009) Matrix crosslinking forces tumor progression by enhancing integrin signaling. *Cell* **139**, 891–906
5. Cox, T. R., Bird, D., Baker, A. M., Barker, H. E., Ho, M. W., Lang, G., and Erler, J. T. (2013) LOX-mediated collagen crosslinking is responsible for fibrosis-enhanced metastasis. *Cancer Res.* **73**, 1721–1732
6. Markolovic, S., Wilkins, S. E., and Schofield, C. J. (2015) Protein hydroxylation catalyzed by 2-oxoglutarate-dependent oxygenases. *J. Biol. Chem.* **290**, 20712–20722
7. Loenarz, C., and Schofield, C. J. (2011) Physiological and biochemical aspects of hydroxylations and demethylations catalyzed by human 2-oxoglutarate oxygenases. *Trends Biochem. Sci.* **36**, 7–18
8. Klose, R. J., Kallin, E. M., and Zhang, Y. (2006) JmjC-domain-containing proteins and histone demethylation. *Nat. Rev. Genet.* **7**, 715–727
9. Peng, J. C., Valouev, A., Swigut, T., Zhang, J., Zhao, Y., Sidow, A., and Wysocka, J. (2009) Jarid2/Jumonji coordinates control of PRC2 enzymatic activity and target gene occupancy in pluripotent cells. *Cell* **139**, 1290–1302
10. Cellot, S., Hope, K. J., Chagraoui, J., Sauvageau, M., Deneault, É., MacRae, T., Mayotte, N., Wilhelm, B. T., Landry, J. R., Ting, S. B., Krosl, J., Humphries, K., Thompson, A., and Sauvageau, G. (2013) RNAi screen identifies Jarid1b as a major regulator of mouse HSC activity. *Blood* **122**, 1545–1555
11. Roesch, A., Fukunaga-Kalabis, M., Schmidt, E. C., Zabierowski, S. E., Brafford, P. A., Vultur, A., Basu, D., Gimotty, P., Vogt, T., and Herlyn, M. (2010) A temporarily distinct subpopulation of slow-cycling melanoma cells is required for continuous tumor growth. *Cell* **141**, 583–594
12. Kottakis, F., Foltopoulou, P., Sanidas, I., Keller, P., Wronski, A., Dake, B. T., Ezell, S. A., Shen, Z., Naber, S. P., Hinds, P. W., McNiel, E., Kuperwasser, C., and Tsichlis, P. N. (2014) NDY1/KDM2B functions as a master regulator of polycomb complexes and controls self-renewal of breast cancer stem cells. *Cancer Res.* **74**, 3935–3946
13. Fadok, V. A., Bratton, D. L., Rose, D. M., Pearson, A., Ezekewitz, R. A., and Henson, P. M. (2000) A receptor for phosphatidylserine-specific clearance of apoptotic cells. *Nature* **405**, 85–90
14. Cui, P., Qin, B., Liu, N., Pan, G., and Pei, D. (2004) Nuclear localization of the phosphatidylserine receptor protein *via* multiple nuclear localization signals. *Exp. Cell Res.* **293**, 154–163
15. Cikala, M., Alexandrova, O., David, C. N., Pröschel, M., Stiening, B., Cramer, P., and Böttger, A. (2004) The phosphatidylserine receptor from Hydra is a nuclear protein with potential Fe(II) dependent oxygenase activity. *BMC Cell Biol.* **5**, 26
16. Chang, B., Chen, Y., Zhao, Y., and Bruick, R. K. (2007) JMJD6 is a histone arginine demethylase. *Science* **318**, 444–447
17. Hong, X., Zang, J., White, J., Wang, C., Pan, C. H., Zhao, R., Murphy, R. C., Dai, S., Henson, P., Kappler, J. W., Hagman, J., and Zhang, G. (2010) Interaction of JMJD6 with single-stranded RNA. *Proc. Natl. Acad. Sci. USA* **107**, 14568–14572

18. Webby, C. J., Wolf, A., Gromak, N., Dreger, M., Kramer, H., Kessler, B., Nielsen, M. L., Schmitz, C., Butler, D. S., Yates III, J. R., Delahunty, C. M., Hahn, P., Lengeling, A., Mann, M., Proudfoot, N. J., Schofield, C. J., and Böttger, A. (2009) Jmjd6 catalyses lysyl-hydroxylation of U2AF65, a protein associated with RNA splicing. *Science* **325**, 90–93
19. Unoki, M., Masuda, A., Dohmae, N., Arita, K., Yoshimatsu, M., Iwai, Y., Fukui, Y., Ueda, K., Hamamoto, R., Shirakawa, M., Sasaki, H., and Nakamura, Y. (2013) Lysyl 5-hydroxylation, a novel histone modification, by Jumonji domain containing 6 (JMJD6). *J. Biol. Chem.* **288**, 6053–6062
20. Wang, F., He, L., Huangyang, P., Liang, J., Si, W., Yan, R., Han, X., Liu, S., Gui, B., Li, W., Miao, D., Jing, C., Liu, Z., Pei, F., Sun, L., and Shang, Y. (2014) JMJD6 promotes colon carcinogenesis through negative regulation of p53 by hydroxylation. *PLoS Biol.* **12**, e1001819
21. Poulard, C., Rambaud, J., Hussein, N., Corbo, L., and Le Romancer, M. (2014) JMJD6 regulates ERα methylation on arginine. *PLoS One* **9**, e87982
22. Gao, W. W., Xiao, R. Q., Peng, B. L., Xu, H. T., Shen, H. F., Huang, M. F., Shi, T. T., Yi, J., Zhang, W. J., Wu, X. N., Gao, X., Lin, X. Z., Dorrestein, P. C., Rosenfeld, M. G., and Liu, W. (2015) Arginine methylation of HSP70 regulates retinoid acid–mediated RARβ2 gene activation. *Proc. Natl. Acad. Sci. USA* **112**, E3327–E3336
23. Böse, J., Gruber, A. D., Helming, L., Schiebe, S., Wegener, I., Hafner, M., Beales, M., Köntgen, F., and Lengeling, A. (2004) The phosphatidylserine receptor has essential functions during embryogenesis but not in apoptotic cell removal. *J. Biol.* **3**, 15
24. Lee, Y. F., Miller, L. D., Chan, X. B., Black, M. A., Pang, B., Ong, C. W., Salto-Tellez, M., Liu, E. T., and Desai, K. V. (2012) JMJD6 is a driver of cellular proliferation and motility and a marker of poor prognosis in breast cancer. *Breast Cancer Res.* **14**, R85; Erratum **19**, 42
25. Poulard, C., Rambaud, J., Lavergne, E., Jacquemetton, J., Renoir, J. M., Trédan, O., Chabaud, S., Treilleux, I., Corbo, L., and Le Romancer, M. (2015) Role of JMJD6 in breast tumourigenesis. *PLoS One* **10**, e0126181
26. Heim, A., Grimm, C., Müller, U., Häußler, S., Mackeen, M. M., Merl, J., Hauck, S. M., Kessler, B. M., Schofield, C. J., Wolf, A., and Böttger, A. (2014) Jumonji domain containing protein 6 (Jmjd6) modulates splicing and specifically interacts with arginine–serine-rich (RS) domains of SR- and SR-like proteins. *Nucleic Acids Res.* **42**, 7833–7850
27. Hu, Y. J., Belaghzal, H., Hsiao, W. Y., Qi, J., Bradner, J. E., Guertin, D. A., Sif, S., and Imbalzano, A. N. (2015) Transcriptional and post-transcriptional control of adipocyte differentiation by Jumonji domain-containing protein 6. *Nucleic Acids Res.* **43**, 7790–7804
28. Sangaletti, S., Di Carlo, E., Gariboldi, S., Miotti, S., Cappetti, B., Parenza, M., Rumio, C., Brekken, R. A., Chiodoni, C., and Colombo, M. P. (2008) Macrophage-derived SPARC bridges tumor cell–extracellular matrix interactions toward metastasis. *Cancer Res.* **68**, 9050–9059
29. Sangaletti, S., Tripodo, C., Sandri, S., Torselli, I., Vitali, C., Ratti, C., Botti, L., Burocchi, A., Porcasi, R., Tomirotti, A., Colombo, M. P., and Chiodoni, C. (2014) Osteopontin shapes immunosuppression in the metastatic niche. *Cancer Res.* **74**, 4706–4719
30. Sangaletti, S., Stoppacciaro, A., Guiducci, C., Torrisi, M. R., and Colombo, M. P. (2003) Leukocyte, rather than tumor-produced SPARC, determines stroma and collagen type IV deposition in mammary carcinoma. *J. Exp. Med.* **198**, 1475–1485
31. Miotti, S., Tomassetti, A., Facetti, I., Sanna, E., Berno, V., and Canevari, S. (2005) Simultaneous expression of caveolin-1 and E-cadherin in ovarian carcinoma cells stabilizes adherens junctions through inhibition of src-related kinases. *Am. J. Pathol.* **167**, 1411–1427
32. Bergamaschi, A., Tagliabue, E., Sørlie, T., Naume, B., Triulzi, T., Orlandi, R., Russnes, H. G., Nesland, J. M., Tammi, R., Auvinen, P., Kosma, V. M., Ménard, S., and Børresen-Dale, A. L. (2008) Extracellular matrix signature identifies breast cancer subgroups with different clinical outcome. *J. Pathol.* **214**, 357–367
33. Ran, F. A., Hsu, P. D., Wright, J., Agarwala, V., Scott, D. A., and Zhang, F. (2013) Genome engineering using the CRISPR-Cas9 system. *Nat. Protoc.* **8**, 2281–2308
34. Zemskov, E. A., Mikhailenko, I., Hsia, R. C., Zaritskaya, L., and Belkin, A. M. (2011) Unconventional secretion of tissue transglutaminase involves phospholipid-dependent delivery into recycling endosomes. *PLoS One* **6**, e19414
35. Yang, H., Chen, Y. Z., Zhang, Y., Wang, X., Zhao, X., Godfroy III, J. I., Liang, Q., Zhang, M., Zhang, T., Yuan, Q., Ann Royal, M., Driscoll, M., Xia, N. S., Yin, H., and Xue, D. (2015) A lysine-rich motif in the phosphatidylserine receptor PSR-1 mediates recognition and removal of apoptotic cells. *Nat. Commun.* **6**, 5717
36. Hehnly, H., Chen, C. T., Powers, C. M., Liu, H. L., and Doxsey, S. (2012) The centrosome regulates the Rab11-dependent recycling endosome pathway at appendages of the mother centriole. *Curr. Biol.* **22**, 1944–1950
37. Zhang, J., Ni, S. S., Zhao, W. L., Dong, X. C., and Wang, J. L. (2013) High expression of JMJD6 predicts unfavorable survival in lung adenocarcinoma. *Tumour Biol.* **34**, 2397–2401
38. Böttger, A., Islam, M. S., Chowdhury, R., Schofield, C. J., and Wolf, A. (2015) The oxygenase Jmjd6—a case study in conflicting assignments. *Biochem. J.* **468**, 191–202
39. Nickel, W., and Rabouille, C. (2009) Mechanisms of regulated unconventional protein secretion. *Nat. Rev. Mol. Cell Biol.* **10**, 148–155 Erratum in: *Nat. Rev. Mol. Cell Biol.* 2009;10:234
40. Hullin-Matsuda, F., Taguchi, T., Greimel, P., and Kobayashi, T. (2014) Lipid compartmentalization in the endosome system. *Semin. Cell Dev. Biol.* **31**, 48–56
41. Hankins, H. M., Sere, Y. Y., Diab, N. S., Menon, A. K., and Graham, T. R. (2015) Phosphatidylserine translocation at the yeast trans-Golgi network regulates protein sorting into exocytic vesicles. *Mol. Biol. Cell* **26**, 4674–4685
42. Rogasevskaia, T. P., and Coorssen, J. R. (2015) The role of phospholipase D in regulated exocytosis. *J. Biol. Chem.* **290**, 28683–28696
43. Giridharan, S. S., Cai, B., Vitale, N., Naslavsky, N., and Caplan, S. (2013) Cooperation of MICAL-L1, syndapin2, and phosphatidic acid in tubular recycling endosome biogenesis. *Mol. Biol. Cell* **24**, 1776–1790, S1–S15
44. Mantri, M., Loik, N. D., Hamed, R. B., Claridge, T. D., McCullagh, J. S., and Schofield, C. J. (2011) The 2-oxoglutarate-dependent oxygenase JMJD6 catalyses oxidation of lysine residues to give 5S-hydroxylysine residues. *Chembiochem* **12**, 531–534
45. Ruoslahti, E., Hayman, E. G., Kuusela, P., Shively, J. E., and Engvall, E. (1979) Isolation of a tryptic fragment containing the collagen-binding site of plasma fibronectin. *J. Biol. Chem.* **254**, 6054–6059
46. Kleinman, H. K., McGoodwin, E. B., Martin, G. R., Klebe, R. J., Fietzek, P. P., and Woolley, D. E. (1978) Localization of the binding site for cell attachment in the alpha1(I) chain of collagen. *J. Biol. Chem.* **253**, 5642–5646
47. Kadler, K. E., Hill, A., and Canty-Laird, E. G. (2008) Collagen fibrillogenesis: fibronectin, integrins, and minor collagens as organizers and nucleators. *Curr. Opin. Cell Biol.* **20**, 495–501
48. Wynn, T. A. (2008) Cellular and molecular mechanisms of fibrosis. *J. Pathol.* **214**, 199–210
49. Tlsty, T. D., and Coussens, L. M. (2006) Tumor stroma and regulation of cancer development. *Annu. Rev. Pathol.* **1**, 119–150
50. Cox, T. R., and Erler, J. T. (2014) Molecular pathways: connecting fibrosis and solid tumor metastasis. *Clin. Cancer Res.* **20**, 3637–3643

Received for publication April 24, 2017.
Accepted for publication July 25, 2017.